Rock seismic anisotropy of the low-velocity zone beneath the volcanic front in the mantle wedge

Katsuyoshi Michibayashi,[1] Tatsuya Oohara,[1] Takako Satsukawa,[1] Satoko Ishimaru,[2] Shoji Arai,[2] and Victor M. Okrugin[3]

[1]Institute of Geosciences, Shizuoka University, Shizuoka 422-8529, Japan

[2]Department of Earth Sciences, Graduate School of Natural Science and Technology, Kanazawa University, Kanazawa 920-1192, Japan

[3]Department of Physical-Chemical Methods of Research and Mineralogy, Institute of Volcanology, Russian Academy of Science, 683006, Petropavlovsk-Kamchatky, Russia

[1] Peridotite xenoliths derived from the low velocity zone beneath the Avacha frontal volcano, Kamchatka, preserve *a*-axis slip fabrics, comparable with those in xenoliths from the back-arc region of the NE Japan. Although low-velocity zones are commonly attributed to zones of partially melted mantle, migration of the melt does not erase the existing olivine fabrics and related seismic anisotropies. These anisotropies may counteract the anisotropies associated with *c*-axis slip fabrics, if they exist, along the slab or in the high-pressure zone.

Key words: rock seismic anisotropy, low-velocity zone, volcanic front, olivine fabric, Avacha, Kamchatka

1. Introduction

[2] Previous studies of various subduction zones have imaged an inclined P- and S-wave low-velocity zone with a velocity reduction of 5–10%, oriented sub-parallel to the down-dip direction of the slab in the mantle wedge [e.g., Northeast Japan: *Zhao et al.*, 1990; Kamchatka: *Gorbatov et al.*, 1999; Tonga: *Conder and Wiens*, 2007]. The low-velocity zone is commonly attributed to a region of partially melted mantle [*Kushiro*, 1987], representing a major source of magma for the volcanic chain that forms along the arc (i.e., the volcanic front). Therefore, the nature of the low-velocity zone represents a

key to understanding the formation of the island-arc above the mantle wedge.

[3] On shear-wave polarization anisotropy in the mantle wedge, whereas the orientation of the fast direction perpendicular to the trench axis on the back-arc region is likely to reflect *a*-axis slip olivine fabrics (A-type) in mantle [e.g., *Nicolas and Christensen*, 1987), the orientation of the fast direction commonly parallel to the trench axis on the fore-arc region might reflect a number of possible mechanisms: deformation of olivine via *c*-axis slip [B-type fabric; *Jung and Karato*, 2001, *Karato*, 2003], trench-parallel flow [e.g., *Smith et al.*, 2001; *Peyton et al.*, 2001], crack induced anisotropy in the crust and/or slab [*Currie et al.*, 2001], or highly anisotropic foliated antigorite serpentine [*Kneller and van Keken*, 2007]. Here, we present that peridotite xenoliths derived from the Avacha frontal volcano, Kamchatka, preserve *a*-axis slip fabrics, comparable with fabrics in xenoliths from the back-arc region. Although low-velocity zones are commonly attributed to zones of partially melted mantle [*Kushiro*, 1987], we infer that migration of the melt does not erase the existing olivine fabric and related seismic anisotropy.

2. Geological settings

[4] The Avacha (=Avachinsky) volcano is part of the frontal chain that forms the volcanic front (VF) of the Kamchatka arc, and is famous for producing peridotite xenoliths derived from the mantle beneath the volcanic front [e.g., *Kepezhinskas et al.*, 1995; *Arai et al.*, 2003; *Ishimaru et al.*, 2007]. The volcano is located in the southern part of the Kamchatka Peninsula, which is a relatively mature arc (Figure 1). The depth to the subducted slab in this region is about 120 km [*Gorbatov et al.*, 1997] and the depth to the Moho is about 37 km [*Levin et al.*, 2002]. The Pacific Plate at this site is subducting relatively rapidly [70–90 mm/year; *Minster et al.*, 1974] beneath the southern part of the Kamchatka Peninsula along the Kuril–Kamchatka trench. In southern Kamchatka, the dip of the subducting plate decreases from 55° to 35° from south to north [*Gorvatov et al.*, 1997], and there occur three sub-parallel volcanic chains at distances from the trench of 200, 320, and 400 km [Figure 1; *Tatsumi et al.*, 1994].

[5] Avacha is a stratovolcano that rises ~2741 m above sea level. Volcanism began in the late Pleistocene and is divided into two stages (IAv and IIAv) based on the chemical composition of ejecta [*Braitseva et al.*, 1998]. IAv is characterized by andesitic pyroclastic flows and tephra over the period 7250 to 3700 years BP, whereas IIAv is

characterized by basaltic andesite lavas extruded from 3500 years BP to the present [*Braitseva et al.*, 1998]. All the effusive rocks are calc-alkaline in chemistry, and some contain megacrystals of hornblende [*Braitseva et al.*, 1998].

3. Samples and Methods

[6] Abundant peridotite xenoliths occur as ejecta (occasionally coated by thin lava film) enclosed in some of the andesitic pyroclastic deposits of IAv [*Braitseva et al.*, 1998]. The xenoliths are subangular to angular in shape and predominantly 5–6 cm (up to 40 cm) across. The grain size of peridotite xenoliths is variable, with some being very-fine-grained, containing olivine crystals less than 1 mm in size [down to 0.1 mm; *Arai et al.*, 2003]. Coarse-grained peridotite xenoliths containing olivine crystals of 1–2 mm in size (maximum size, 10 mm) are the main focus of this study, since they are a good representation of the seismic properties of the mantle wedge as described below. We analyzed 16 peridotite xenoliths to evaluate the effect of rock seismic properties on seismic-wave properties, focusing on three common minerals: olivine, orthopyroxene, and clinopyroxene, of which olivine is the most common mineral in the upper mantle.

[7] Most of the xenoliths from Avacha are spinel harzburgites, with subordinate pyroxenites (clinopyroxenite and orthopyroxenite), dunite, and hornblende-gabbros; the host rock is basaltic andesite. Based on petrological data, the peridotite xenoliths are thought to have originated from depths shallower than 60 km [*Arai et al.*, 2003]. Given that the depth to the Moho in this area is about 37 km, the peridotite xenoliths are likely to have originated in the uppermost 20 km of the mantle beneath Avacha volcano. The xenoliths record temperatures of 800–1050 °C, as indicated by Ca contents in orthopyroxene [*Brey and Köhler*, 1990]. These temperatures could reflect the temperature gradient of the uppermost mantle beneath the volcanic front [*Ishimaru et al.*, 2007]; consequently, we infer that the peridotite xenoliths were derived from the uppermost part of the low-velocity zone in the mantle.

[8] The peridotite xenoliths contain a pervasive main foliation and a lineation defined by aligned spinel crystals. We analyzed microstructures from thin sections cut perpendicular to the foliation and parallel to the lineation (i.e., XZ sections). The peridotite xenoliths have a coarse-grained granular texture and contain elongate olivine grains. All of the peridotite xenoliths share a common texture, indicating an origin related to a pervasive event in the uppermost mantle beneath the volcanic front. Olivine crystals

have a shape-preferred orientation oblique to the main foliation by 0–30°. Such an oblique foliation is typical of shear deformation and has been reported from rocks of the uppermost mantle of the back-arc region (Ichinomegata peridotite xenoliths, Northeast Japan) [*Michibayashi et al.*, 2006]. Hence, from the 16 xenoliths data with each one containing more than 200 measurements, we calculated the average sample (4325 measurements, the sum of all the measurements with respect to the same sense of shear based on each oblique foliation), giving the same weight to each measurement, independently of the number of measurements in each xenolith (Figure 2A).

[9] We calculated the seismic properties of the peridotite xenoliths based on single-crystal elastic constants, crystal density, the average crystal-preferred orientations (CPOs) of olivine, enstatite, and diopsite, and the average modal composition of these three minerals (Figure 2A). The elastic constants used in our calculations are those of *Abramson et al.* [1997] for olivine, *Chai et al.* [1997] for enstatite, and *Collins and Brown* [1998] for diopside; we also used the Voigt–Reuss–Hill averaging scheme [*Mainprice et al.*, 2000].

4. Results

[10] The P-wave velocity is fastest (8.61 km/s) subparallel to the lineation and is closely related to the CPO maximum of olivine [100] (Figure 2A). The P-wave velocity is slow (8.12 km/s) for waves propagating in a plane normal to the [100] maximum, resulting in an axial symmetry with the [100] maximum as the symmetry axis. Polarization anisotropies have maxima girdles on each side of a plane normal to the [100] maximum, whereas the minimum birefringence (0.04%) occurs for propagation directions close to the [100] maximum, subparallel to the lineation (Figure 2A). The orientation of the polarization plane of the fastest S-wave marks the orientation of the great circle that contains the maximum concentration of [100] (Figure 2A).

5. Discussion

[11] Although the original orientations of the peridotite xenoliths were lost during their volcanic transport to the surface, we are able to derive quantitative constraints on the intrinsic anisotropy within the lithospheric mantle. The thickness (T) of an anisotropic layer is given by T = (100dt<Vs>)/AVs, where dt is the delay time of S-waves, <Vs> is the average velocity of the fast and slow velocities, and AVs is the anisotropy for a

specific propagation direction expressed as a percentage [e.g., *Pera et al.*, 2004]. Accordingly, we estimated an anisotropic layer of 13–38 km thickness to explain the observed local-S fast-polarization axes with splitting delays of 0.1–0.3 s [at PET in Figure 1; *Peyton et al.*, 2001; *Levin et al.*, 2004], indicating that the intrinsic rock seismic anisotropy is sufficient to generate the observed delay time.

[12] *Levin et al.* [2004] showed that the orientation of the local-S fast-polarization is normal to the trench axis in the vicinity of the Avacha volcano, which is consistent with the observed fabrics of the peridotite xenoliths defined by *a*-axis slip olivine CPO patterns (Figure 2). The profile A of *Gorbatov et al.* [1999] clearly shows a Vp slow (-7 to -3 %) anomaly below the volcanic front at PET from surface down to 90 km depth. Such reduction of Vp % can be for instance explained by the occurrence of 10 to 5 % spherical melt pocket [*Mainprice*, 1997]. Consequently, the seismic P-wave observations of *Gorbatov et al.* [1999] combined with S-wave results of *Levin et al.* [2004] suggest that melt is present to explain the low P-wave speed, while *a*-axis slip olivine fabric is present to explain the S-wave anisotropy, at least locally at PET. It is additionally noted that *a*-axis slip olivine fabrics within peridotite xenoliths has been also tentatively reported from Iraya frontal volcano, Philippines [*Arai et al.*, 2004].

[13] The obtained rock seismic properties are comparable to those reported from the back-arc region of the uppermost mantle in the Northeast Japan arc [Figure 2B; *Michibayashi et al.*, 2006]. The Northeast Japan arc is the southwestward extension of the Kamchatka arc, where the Pacific Plate subducts beneath the North American Plate; accordingly, it is possible that the structure of the mantle wedge is identical in the two arcs (Figure 3). This is also consistent with a seismic study in the Northeast Japan, where the fast propagation axis of P-waves is in mostly E-W direction in the mantle wedge [*Ishise and Oda*, 2005]. Such a scenario would indicate that although low-velocity zones are commonly attributed to zones of partially melted mantle, the migration of melt does not erase the existing CPO and related seismic anisotropy, which are similar to those found in back-arc peridotites (Figure 2).

[14] In contrast, the orientation of the local-S fast polarization commonly changes from the trench-normal to the trench-parallel at around the volcanic front [e.g., the northeast Japan; *Nakajima and Hasegawa*, 2004]. Therefore, the observed anisotropy may result from other factors such as *c*-axis slip olivine fabrics (B-type) along the slab [*Jung and Karato*, 2001; *Katayama and Karato*, 2006] and/or in the high-pressure zone

[*Jung et al.*, 2009], the alignment of melt lenses in the low-velocity zone, or cracks with fluid infill. Recently, *Katayama* [2009] argued that the seismic anisotropy induced by olivine fabrics could result from a thin layer along the slab and overriding plate. Whereas the olivine fabrics may be B-type along the slab as documented by *Mizukami et al.* [2004], *Skemer et al.* [2006] and *Tasaka et al.* [2008], our results argue that the seismic properties induced by B-type fabrics along the slab are counteracted by those induced by *a*-axis slip olivine fabrics in the uppermost mantle of the overriding plate beneath the volcanic front (Figure 3), as the two slip systems produce similar degrees of rock seismic anisotropy [compare Figure 2 with *Tasaka et al.*, 2008]. Therefore, other factors such as melt alignment in the low-velocity zone or cracks with fluid infill might represent the more likely explanation of the observed seismic anisotropy in the vicinity of the volcanic front.

[15] **Acknowledgements.** Part of the samples analyzed in this work were collected by K. Kadoshima and A. Koyanagi during fieldwork undertaken in 2000 and the rest were collected by SI, SA and VMO. This manuscript was significantly improved through constructive reviews by D. Mainprice and P. Skemer. This study was supported by research grants from the Japan Society for the Promotion of Science (Nos. 16340151 and 19340148) awarded to KM and Gran-in-Aid for Scientific Research (No. 13440161) and the 21st Century COE project (led by Prof. K. Hayakawa) to SA.

References

Abramson, E. H., J. M. Brown, L. J. Slutsky, and J. J. Zang (1997), The elastic constants of San Carlos olivine to 17 GPa, *J. Geophys. Res.*, *102*, 12,253–12,263.

Arai, S., S. Takada, K. Michibayashi, and M. Kida (2004), Petrology of peridotite xenoliths from Iraya Volcano, Philippines, and its implication for dynamic mantle-wedge processes, *J. Petrol.*, 45, 369-389.

Arai, S., S. Ishimaru, and V. M. Okrugin (2003), Metasomatized harzburgite xenoliths from Avacha volcano as fragments of mantle wedge of the Kamchatka arc: implication for the metasomatic agent, *Island Arc*, *12*, 233–246.

Braitseva, O. A., L. I. Bazanova, I. V. Melekestsev, and L. D. Sulerzhitskiy (1998), Large Holocene eruptions of Avacha volcano, Kamchatka (7200-3500 14C years B.P.), *Volcanology and Seismology*, *20*, 1–27.

Brey, G. P. and T. Köhler (1990), Geothermobarometry in four-phase lherzolite II. New thermobarometers, and practical assessment of existing thermobarometers, *J. Petrol.*, *31*, 1353–1378.

Chai, M., J. M. Brown, L. J. Slutsky, and J. Zang (1997), The elastic constants of an aluminous orthopyroxene to 12.5 GPa, *J. Geophys. Res.*, *102*, 14779–14785.

Collins, M. D. and J. M. Brown (1998), Elasticity of an upper mantle clinopyroxene, *Phys. Chem. Min., 26,* 7–13.

Conder, J. A. and D. A. Wiens (2007), Rapid mantle flow beneath the Tonga volcanic arc, *Earth Planet. Sci. Lett.*, *264*, 299–307.

Currie, C. A., J. F. Classidy, and R. D. Hyndman (2001), A regional study of shear wave splitting above the Cascadia subduction zone: margin-parallel crustal stress, *Geophys. Res. Lett.*, *28*, 659–662.

Gorbatov, A., V. Kostoglodov, G. Suarez, and E. Gordeev (1997), Seismicity and structure of the Kamchatka subduction zone, *J. Geophys. Res.*, *102*, 17883–17898.

Gorbatov, A., J. Dominguez, G. Suarez, V. Kostoglodov, D. Zhao, and E. Gordeev (1999), Tomographic imaging of the P-wave velocity structure beneath the Kamchatka peninsula, *Geophys. J. Int.*, *137*, 269–279.

Ishimaru, S., S. Arai, Y. Ishida, M. Shirasaka, and V. M. Okrugin (2007), Melting and multi-stage metasomatism in the mantle wedge beneath a frontal arc inferred from highly depleted peridotite xenoliths from the Avacha volcano, southern Kamchatka, *J. Petrol.*, *48*, 395–433.

Ishise, M. and H. Oda (2005), Three-dimensional structure of *P*-wave anisotropy beneath the Tohoku district, northeast Japan, *J. Geophys. Res.*, *110*, B07304, doi:10.1029/2004JB003599.

Jung, H. and S. Karato (2001), Water-induced fabric transitions in olivine, *Science*, *293*, 24–27.

Jung, H., W. Mo, and H. W. Green (2009), Upper mantle seismic anisotropy resulting from pressure-induced slip transition in olivine, *Nature Geoscience*, *2*, 73–77.

Katayama, I. (2009), Thin anisotropic layer in the mantle wedge beneath northeast Japan, *Geology*, *37*, 211-214.

Katayama, I. and S. Karato (2006), Effect of temperature on the B- and C-type olivine fabric transition and implication for flow pattern in subduction zones, *Phys. Earth Planet. Inter.*, *157*, 33–45.

Kepezhinskas, P. K., M. J. Defant, and M. S. Drummond (1995), Na metasomatism in the island-arc mantle by slab melt-peridotite interaction; evidence from mantle xenoliths in the North Kamchatka arc, *J. Petrol.*, *36*, 1505–1527.

Kneller, E.A. and P. E. van Keken (2007), Trench-parallel flow and seismic anisotropy in the Mariana and Andean subduction systems, *Nature*, *450*, 1222–1225.

Kushiro, I. (1987), A petrological model of the mantle wedge and lower crust in the Japanese island arcs, *The Geochemical Society, Special Publication No. 1*, 165–181.

Levin, V., I. Park, M. Brandon, J. Lees, V. Peyton, E. Gordeev, and A. Ozerov (2002), Crust and upper mantle of Kamchatka from teleseismic receiver functions, *Tectonophysics*, *358*, 233–265.

Levin, V., D. Droznin, J. Park, and E. Gordeev (2004), Detailed mapping of seismic anisotropy with local shear waves in southeastern Kamchatka, *Geophys. J. Int.*, *158*, 1009–1023.

Mainprice, D. (1997), Modelling the anisotropic seismic properties of partially molten rocks found at mid-ocean ridges, *Tectonophysics*, *279*, 161-179.

Mainprice, D., G. Barruol, W. Ben Ismaïl (2000), The anisotropy of the Earth's mantle: from single crystal to polycrystal, in: S. Karato, A.M. Forte, R.C. Liebermann, G. Masters, L. Stixrude (Eds.), Mineral Physics and Seismic Tomography: From Atomic to Global, AGU Geophysical Monograph, vol. 117, pp. 237–264.

Michibayashi, K., N. Abe, A. Okamoto, T. Satsukawa, and K. Michikura (2006), Seismic anisotropy in the uppermost mantle, back-arc region of the northeast Japan arc: Petrophysical analyses of Ichinomegata peridotite xenoliths, *Geophys. Res. Lett.*, *33*, doi:10.1029/2006GL025812.

Minster, J. B., T. H. Jordan, P. Molnar, and E. Haines (1974), Numerical modelling of instantaneous plate tectonics, *Geophys. J.*, 36, 541–576.

Nakajima, J. and A. Hasegawa, (2004), Shear-wave polarization anisotropy and subduction-induced flow in the mantle wedge of northeastern Japan, *Earth Planet. Sci. Lett.*, *225*, 365–377.

Nicolas, A., and N. I. Christensen (1987), Formation of anisotropy in upper mantle peridotite: a review, in: K. Fuchs, C. Froidevaux (Eds.), Composition Structure and Dynamics of the Lithosphere–Asthenosphere System, Geodyn. Monogr. Ser., AGU, Washington, D. C., 111–123.

Pera, E., D. Mainprice, and L. Burlini (2004), Anisotropic seismic properties of the upper mantle beneath the Torre Alfina area (northern Apennines, central Italy), Tectonophysics, 370, 11 –30.

Peyton, V., V. Levin, J. Park, M. Brandon, J. Lees, E. Gordeev, and A. Ozerov (2001), Mantle flow at a slab edge: seismic anisotropy in the Kamchatka region, *Geophys. Res. Lett.*, *28*, 379–382.

Smith, P. G., D. A. Wiens, K. M. Fischers, L. M. Dorman, S. C. Webb, and J. A. Hildebrand (2001), A complex pattern of mantle flow in the Lau backarc, *Science*, *292*, 713–716.

Skemer, P., I. Katayama, S. Karato (2006), Deformation fabrics of the Cima di Gagnone peridotite massif, Central Alps, Switzerland: evidence of deformation at low temperatures in the presence of water, *Contri. Mineral. Petrol.*, *152*, 43–51.

Tasaka, M., K. Michibayashi, and D. Mainprice (2008), B-type olivine fabrics developed in the fore-arc side of the mantle wedge along a subducting slab, *Earth Planet. Sci. Lett.*, *272*, 747–757.

Tatsumi, Y., Y. Furukawa, T. Kogiso, Y. Yamanaka, T. Yokoyama, and S. A. Fedetov (1994), A third volcanic chain in Kamchatka: thermal anomaly at transform/convergence plate boundary, *Geophys. Res. Lett.*, 21, 537–540.

Zhao, D., S. Horiuchi, and A. Hasegawa (1990), 3-D seismic velocity structure of the crust and the uppermost mantle in the northeastern Japan Arc, *Tectonophysics*, *181*, 135–149.

Figure 1. Location of the Avacha volcano. Map of the Kamchatka region shows the contours of the Wadati-Benioff zone (adapted from Gorbatov et al., 1997), and the location of the three volcanic chains from Tatsumi et al. (1994). PET is Petropavlovsk-Kamchatsky, the capital city of Kamchatka. VF: volcanic front.

Figure 2. Olivine crystallographic preferred orientations (CPOs) and seismic properties computed from single crystal elastic constants, crystal density, and the average CPOs of olivine, enstatite, and diopsite. Contours are multiples of uniform density. Foliation is horizontal (XY plane; solid line), and the lineation (X) is oriented E-W within the plane of the foliation. Vp: 3D distribution of the P-wave velocity. Contours are multiples of the uniform density. Anisotropy is (Vpmax−Vpmin)/Vpmean. AVs: 3D distribution of the polarization anisotropy of S-waves owing to S-wave splitting. Vs1 plane: polarization plane of the fast split S-wave (S1) as a function of the orientation of the incoming wave relative to the structural frame (X, Y, Z) of the sample. Each small segment on the figure represents the trace of the polarization plane on the point at which S1 penetrates the hemisphere. Color shading for AVs is also shown on the figure. (A) Olivine CPOs and seismic properties of Avacha peridotite xenoliths derived from the frontal volcano of the Kamchatka arc. See Fig. 1. (B) Seismic properties of Ichinomegata peridotite xenoliths derived from the back-arc region of the Northeast Japan arc.

Figure 3. Schematic cross section of the mantle wedge in the West Pacific margin. The rock seismic anisotropies are similar along the uppermost mantle due to a-axis slip fabrics (green color), whereas the fast-direction of S-wave anisotropy may change at the volcanic front.

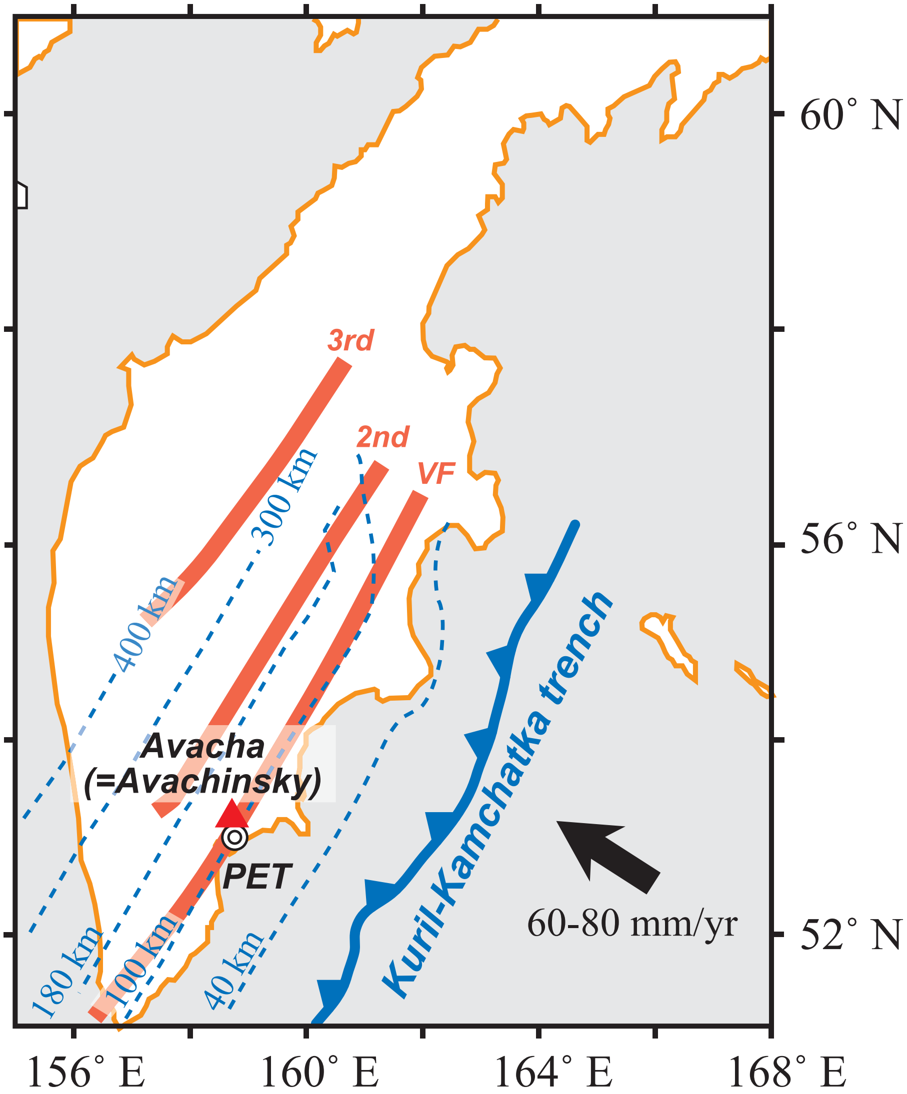

3rd
2nd
VF
300 km
400 km
180 km
100 km
40 km
Avacha
(=Avachinsky)
PET
Kuril-Kamchatka trench
60-80 mm/yr
60° N
56° N
52° N
156° E
160° E
164° E
168° E

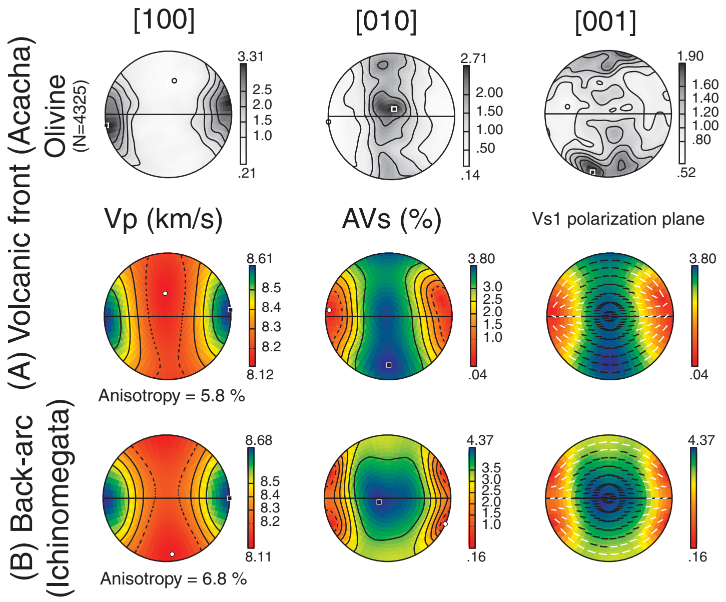
[100]
[010]
[001]
Olivine
(N=4325)
(A) Volcanic front (Acacha)
3.31
2.5
2.0
1.5
1.0
.21
2.71
2.00
1.50
1.00
.50
.14
1.90
1.60
1.40
1.20
1.00
.80
.52
Vp (km/s)
AVs (%)
Vs1 polarization plane
8.61
8.5
8.4
8.3
8.2
8.12
Anisotropy = 5.8 %
3.80
3.0
2.5
2.0
1.5
1.0
.04
3.80
.04
(B) Back-arc
(Ichinomegata)
8.68
8.5
8.4
8.3
8.2
8.11
Anisotropy = 6.8 %
4.37
3.5
3.0
2.5
2.0
1.5
1.0
.16
4.37
.16

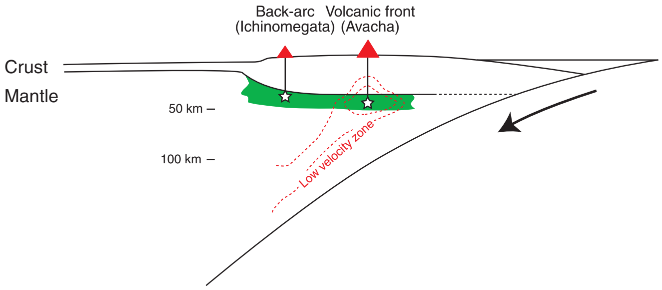
Back-arc
(Ichinomegata)
Volcanic front
(Avacha)
Crust
Mantle
50 km
100 km
Low velocity zone